Néel order, quantum spin liquids, and quantum criticality in two dimensions

Pouyan Ghaemi[1] and T. Senthil[1,2]
[1]*Department of Physics, Massachusetts Institute of Technology, Cambridge, Massachusetts 02139, USA*
[2]*Center for Condensed Matter Theory, Indian Institute of Science, Bangalore 560012, India*
(Received 27 September 2005; published 10 February 2006)

This paper is concerned with the possibility of a direct second-order transition out of a collinear Néel phase to a paramagnetic spin liquid in two-dimensional quantum antiferromagnets. Contrary to conventional wisdom, we show that such second-order quantum transitions can potentially occur to certain spin liquid states popular in theories of the cuprates. We provide a theory of this transition and study its universal properties in an ϵ expansion. The existence of such a transition has a number of interesting implications for spin-liquid-based approaches to the underdoped cuprates. In particular it considerably clarifies existing ideas for incorporating antiferromagnetic long range order into such a spin-liquid-based approach.

DOI: 10.1103/PhysRevB.73.054415 PACS number(s): 75.10.Jm, 74.20.Mn, 75.40.Cx, 76.50.+g

I. INTRODUCTION

In recent years a number of old ideas on theories of the cuprate materials have been clarified and rejuvenated. A variety of experiments now support the notion that the underdoped cuprates are usefully regarded as doped Mott insulators—in other words proximity to the Mott insulator strongly influences the properties of the underdoped materials.[1] The undoped Mott insulating parent materials have long-range antiferromagnetic order. However, this order disappears rather quickly upon doping. Rather (at not too low temperatures) the pseudogap state that appears above the superconducting transition in the underdoped materials is probably best regarded as a doped version of a *paramagnetic* Mott insulator. Such an insulator has a "built-in" spin (pseudo)gap. Vexing questions, however, remain on the precise theoretical connection between such a point of view and the actual occurrence of antiferromagnetic order in the underdoped materials.

A clue to resolving this dilemma is provided by neutron scattering experiments that reveal the existence of a sharp magnetic resonance at (π,π) in the doped superconductor.[2–4] An appealing interpretation of this resonance is as a gapped version of the familiar magnon of a proximate antiferromagnetic state.[5–7] Interestingly, as the doping is reduced, the resonance frequency goes down proportionately to T_c.[8,9] This suggests that if the doped state is to be viewed as a doped paramagnet, then the latter may at least be connected to the Néel state by a second-order transition (see Fig. 1). Thus we are led to search for quantum paramagnetic states of spin-1/2 moments on a square lattice that are accessible from the collinear Néel state by a second-order transition.

It is important at this point to also review another old idea in cuprate theory. Early work[10,11] suggested that the undoped magnetically ordered Mott insulator is close to being disordered by quantum fluctuations into a paramagnetic featureless "spin liquid" phase. Such a spin liquid state was postulated to have neutral spin-1/2 spinon excitations and preserve all the symmetries of the underlying microscopic spin Hamiltonian (including spin rotation). Further, it was argued that doping a spin liquid could possibly lead to high-temperature superconductivity.[10,11]

Despite its original appeal, this scenario was subsequently questioned by a number of significant theoretical developments. Calculations in a controlled large-N expansion of quantum Heisenberg spin models concluded that the natural result of destruction of collinear Néel order was not a featureless spin liquid but (for spin 1/2) a valence bond solid (VBS), which breaks various lattice symmetries.[12] (Here natural refers to the possibility that the quantum paramagnet in question is potentially separated from the Néel state by a second-order transition.) The VBS state also does not support fractionalized spinon excitations. This was supported by a number of other indirect arguments—for instance by studies of quantum dimer models on the square lattice.[13] It was shown, however, that destruction of noncollinear Néel order could indeed lead to a fractionalized spin liquid state that preserves all lattice symmetries.[14]

These calculations lead to the following folk wisdom (for a review, see Ref. 15): "In two spatial dimensions collinear ordered magnets naturally give way to confined VBS paramagnets when disordered by quantum fluctuations while noncollinear magnets naturally lead to spin liquids." As the magnetic ordering is undoubtedly collinear in the cuprates

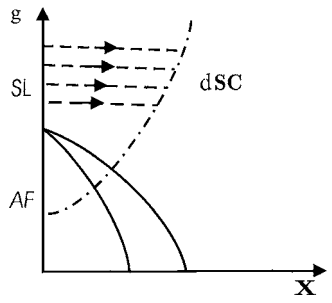

FIG. 1. Zero-temperature phase diagram showing the route from Mott insulating antiferromagnet to *d*-wave superconductor (dash-dotted line). Horizontal axis refers to doping and vertical axis refers to frustrating spin interactions that destabilize the Néel state. The thesis of the spin liquid approach is that the intermediate- and long-scale physics of the doped system may be fruitfully viewed as those of a doped spin liquid Mott insulator. Doping the spin liquid phase naturally leads to a *d*-wave superconducting state (dashed lines).

this folk wisdom apparently spells doom for the view of the cuprates as doped spin liquid paramagnetic Mott states.

The purpose of the present paper is to reconsider these issues. We will first argue that, if at all a spin-liquid-based approach is to be pursued, experiments suggest a certain kind of paramagnetic spin liquid state as natural candidate "parent" states of the doped cuprates. Next we argue that the existing theoretical work does not rule out a direct second-order transition between the Néel state and this particular kind of spin liquid state. Finally we outline in some detail a theory for just such a direct second-order transition. Thus our work calls into question the folklore described above and potentially frees the spin-liquid-based approach to the cuprates from one of its theoretical criticisms.

Based on these results we will develop a qualitative picture of the neutron resonance mode seen in experiments in the doped system and its relationship with other aspects of the observed spin physics. Our description will naturally unify two popular views of the resonance mode—one as a soft mode associated with antiferromagnetic long-range order,[5–7] and the other as a spin exciton formed as a triplet particle-hole collective mode of fermionic quasiparticles.[16–20]

We begin with experiments. It is by now quite clearly established that the cuprate superconductors are *d*-wave paired and furthermore have nodal BCS-like quasiparticles. The existence of the nodal quasiparticles is theoretically significant. Indeed the possibility of *d*-wave paired superconductors without nodal quasiparticles has been much emphasized by Kivelson and co-workers (for a review see Ref. 21). It is therefore of some interest to ask whether there exist paramagnetic Mott states that already have gapless nodal excitations. Such a state then builds in enough of the spin physics seen in the experiments at finite doping that it would be an attractive parent Mott insulator as a basis for a theory of the underdoped cuprates.

Remarkably such states are known to exist as stable quantum phases[22,23] of quantum antiferromagnets on a two-dimensional square lattice, at least within an appropriate large-*N* expansion. In this paper we will focus on one such state that has played a central role in some previous theoretical work[24–29] on the cuprate problem. This state—dubbed the *d*-wave resonating valence band (*d*RVB) or staggered flux (sF) spin liquid—is a quantum paramagnet that nevertheless has gapless spin-carrying excitations. Recent theoretical work[23] has established the stability of such a state (in a suitable large-*N* expansion). A low-energy description of the physics is usefully provided in terms of a theory of gapless nodal fermionic spinons coupled minimally to a fluctuating U(1) gauge field. Despite this, however, there really is no true quasiparticle description of the low-energy spectrum.[28,30]

In this paper we are interested in exploring the quantum phase transition between this algebraic spin liquid and the collinear Néel state. Previous theoretical work providing the basis for the folk wisdom mentioned above does not constrain the nature of this transition. First the large-*N* calculations of Ref. 12 were based on a bosonic representation of the spins. This representation is not well suited to access the algebraic spin liquid phase. Indeed it is tailor made to access either VBS phases or gapped spin liquids with bosonic spinons. Arguments for the presence of VBS order in the paramagnet based on quantum dimer models on the square lattice[13] also do not help. Clearly the quantum dimer models are useful only for paramagnets with a full spin gap—and hence will not be able to access algebraic spin liquids (ASLs). A more recent elegant argument[31] attacks from the spin liquid side as follows. First it supposes that to access Néel-ordered states from spin liquids, the latter must have bosonic spinons. Then the Néel state is reached simply by condensing the bosons. Examining the dispersion relation of a bosonic spinon in a spin liquid state reveals that it generically has a minimum at an incommensurate wave vector. Condensing such a spinon then naturally leads to incommensurate spiral states and not to the simple collinear state. A loophole in this argument is the supposition that it is only a spin liquid state with bosonic spinons that can be proximate (i.e., separated by a second-order transition) to a Néel state. Indeed we will show in this paper that the algebraic spin liquid state—which does not have bosonic spinons—can be connected to the Néel state by a second-order transition.

Our starting point is a mean-field description of both the spin liquid and antiferromagnetic phases. This will be done in terms of a slave particle representation of the spin operator in terms of neutral fermionic spinons. At this mean-field level the spin liquid state we study will have spinons that are paired into a *d*-wave state. The resulting spinon dispersion has four Fermi points in the Brillouin zone at which the spinons are gapless. Antiferromagnetism is obtained in this representation as a spin density wave transition of the spinons. This magnetic ordering produces a gap for the spinons. Such a mean-field description of the antiferromagnetic state was first proposed by Hsu.[32] Similar ideas have subsequently been explored in a number of publications—see Refs. 33–36. However, it is important to realize that the resulting mean-field state is not a conventional antiferromagnet. Though the spinons have acquired a gap they still have not disappeared from the spectrum. Thus the mean-field description is apparently that of a *fractionalized* antiferromagnet. For the particular mean-field state studied in this paper this problem is cured once fluctuations beyond the mean field are included. Indeed, we will argue that these fluctuations confine the spinons in the magnetically ordered state.

Does the slave particle mean-field description of the antiferromagnet still have any physical meaning if the spinons are confined? An answer to this question is provided by considering the magnetic state close to the transition to the spin liquid. The critical point we describe for this transition has some conceptual similarity with the deconfined quantum critical points[37,38] studied recently. Specifically, spinon variables will already prove useful in describing the critical point itself though they do not correspond to physical degrees of freedom deep in the Néel phase. (See Fig. 2.) Furthermore there are two diverging length and time scales—one of which diverges as a power of the other—as the transition is approached from the Néel side. The physics is that of the conventional Néel state only at the very longest scales. At length and time scales intermediate between the two diverging ones, the physics is correctly thought of in terms of the mean-field spin density wave state formed out of fermionic

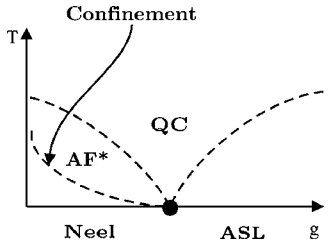

FIG. 2. Schematic phase diagram of quantum phase transition between Néel and *d*RVB algebraic spin liquid phases.

Dirac-like spinons. This state (though ultimately unstable) describes an increasingly wider regime of intermediate scales close to the transition. Apart from the spin waves expected from broken spin symmetry it also contains gapped spin-1/2 spinons coupled minimally to a gapless spin-0 gauge boson (a "photon"). Thus in this large intermediate-scale regime the spinon mean-field description of the antiferromagnet is indeed the correct physical starting point. Note that accessing the true critical theory requires keeping fluctuations other than those of the Néel order parameter. This should hardly be a surprise given the nontrivial nature of the paramagnetic phase.

The rest of the paper is organized as follows. In Sec. II we quickly outline the mean-field theory of the spin liquid and the transition to the Néel state. Next in Sec. III we go beyond mean field, by including gauge fluctuation for spinons and dynamics for the Néel field. We first briefly review the properties of the algebraic spin liquid phase with particular emphasis on precursor fluctuations of the magnetic ordering near the transition (Sec. III A). Then in Sec. III B we discuss the magnetic state and show that it gets smoothly connected to the conventional Néel state once monopole fluctuations are included. We very briefly discuss the connection to projected wave function descriptions of the magnetism in undoped spin models in Sec. III C. Next in Sec. IV we consider the phase transition. We show that within certain assumptions the transition has a conceptually similar structure to the deconfined critical points of Ref. 37. We then present results for both the ASL phase and the transition to the Néel state within an appropriate ϵ expansion in Sec. V. In Sec. VI we discuss implications of our results for theories of cuprates before concluding in Sec. VII. Various appendixes contain technical details of the calculations.

II. MEAN-FIELD THEORY

Consider a generic SU(2) symmetric spin-1/2 model on a square lattice with predominantly antiferromagnetic short-ranged interactions:

$$\mathcal{H} = J \sum_{<rr'>} \vec{S}_r \cdot \vec{S}_{r'} + \cdots . \tag{1}$$

Here $J>0$ (antiferromagnetic exchange), and the ellipsis represents frustrating interactions that can be used to tune quantum phase transitions. We will require that the full Hamiltonian be invariant under SU(2) spin rotations, time reversal, and the full space group of the square lattice. It is well known that the nearest neighbor model has a Néel-ordered ground state. Various paramagnetic ground states can be accessed (in principle) by appropriate frustrating interactions. As explained in the Introduction, here we will focus on a particular paramagnetic state that is known as the *d*RVB algebraic spin liquid (also often referred to as the staggered flux spin liquid). A mean-field theory for this state has been described several times in the literature and is well known.[24] First the spin is formally rewritten as a bilinear of fermionic "spinon" operators

$$\vec{S}_r = \frac{1}{2} f^\dagger_{r\alpha} \vec{\sigma}_{\alpha\beta} f_{r\beta}. \tag{2}$$

Here $\alpha=1,2$, corresponding to spin-up or spin-down fermions. This is an exact rewriting when combined with the local constraint $f^\dagger_\alpha f_\alpha = 1$. In the mean-field approximation the exact Hamiltonian is replaced by one quadratic in the spinon operators but with self-consistently determined parameters. For the *d*RVB state, the mean-field Hamiltonian takes the form

$$H_{SF} = -\sum_{\langle rr' \rangle} [(\chi_{rr'} + i\Delta_{rr'}) f^\dagger_r f_{r'} + \text{H.c.}]. \tag{3}$$

Here we take r to belong to one sublattice of the square lattice, so that r' belongs to the opposite sublattice. The constants $\Delta_{rr'} = +\Delta$ on horizontal bonds and $-\Delta$ on vertical bonds while $\chi_{rr'} = t$ on all bonds. This describes fermionic spin-1/2 spinons on the square lattice with complex hopping amplitudes such that there is a nonzero flux that is staggered from plaquette to plaquette. Despite appearances, this saddle point possesses the full symmetry of the microscopic model including all lattice symmetries. (The apparent breaking of translational symmetry is a gauge artifact.) Recent work has clarified the nature of fluctuations about this mean-field state. But in this present section, we will stick to the mean-field description and see how a transition to a Néel-ordered state may be described.

To access a Néel state we modify the *d*RVB mean-field Hamiltonian by adding a nearest neighbor antiferromagnetic interaction between the spinons. Such an interaction will anyway be induced once fluctuations beyond the mean-field theory are considered. By including it explicitly, we can induce a spin density wave ordering of the fermionic spinons. We therefore consider

$$H = -\sum_{\langle rr' \rangle} (T_{rr'} f^\dagger_r f_{r'} + T^*_{rr'} f^\dagger_{r'} f_r) + \frac{1}{g} \sum_{\langle rr' \rangle} \vec{S}_r \cdot \vec{S}_{r'}. \tag{4}$$

Here $T_{rr'} = T = t + i\Delta$ on bonds as shown in Fig. 3 and equals $T^* = t - i\Delta$ on other bonds as also shown in Fig. 3. We now treat the $1/g$ term in a mean-field approximation. We look for a solution where $\langle \vec{S}_r \rangle = \epsilon_r N \hat{z}$ is nonzero (in mean-field theory, $\vec{N} = \langle \epsilon_r \vec{S}_r \rangle$ is constant; so we can choose its direction as the z direction). Here $\epsilon_r = (-1)^{x+y}$ is $+1$ on the A sublattice and -1 on the B sublattice. The mean-field Hamiltonian reads

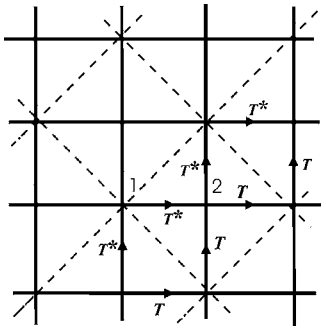

FIG. 3. Two-site unit cells (indicated by dashed lines) used to diagonalize the mean-field Hamiltonian.

$$H_{MF} = -\sum_{\langle rr' \rangle} (T f_r^\dagger f_{r'} + T^* f_{r'}^\dagger f_r) - \frac{4N}{g} \sum_r \epsilon_r f_r^\dagger \frac{\sigma^z}{2} f_r. \quad (5)$$

The value of N is to be determined self-consistently. We can diagonalize this Hamiltonian using a two-site unit cell as plotted in Fig. 3. This gives the following equation for energy eigenvalues and eigenstates:

$$\begin{bmatrix} -\frac{4}{g} N \frac{\sigma^z}{2} & \varepsilon(\mathbf{k}) - i\Delta(\mathbf{k}) \\ \varepsilon(\mathbf{k}) + i\Delta(\mathbf{k}) & \frac{4}{g} N \frac{\sigma^z}{2} \end{bmatrix} \begin{bmatrix} f_1 \\ f_2 \end{bmatrix} = E_{\mathbf{k}} \begin{bmatrix} f_1 \\ f_2 \end{bmatrix}. \quad (6)$$

Here, f_1 belongs to one sublattice and f_2 to the other one. We have decomposed T as $t - i\Delta$. $\varepsilon(\mathbf{k})$ and $\Delta(\mathbf{k})$ are then defined as

$$\varepsilon(\mathbf{k}) = -2t[\cos(k_y) + \cos(k_x)],$$

$$\Delta(\mathbf{k}) = 2\Delta[\cos(k_x) - \cos(k_y)].$$

This gives the spectrum of the two bands:

$$E_{\mathbf{k}}^{\pm} = \pm \sqrt{\left(\frac{2N}{g}\right)^2 + \varepsilon(\mathbf{k})^2 + \Delta(\mathbf{k})^2}. \quad (7)$$

Now with this in hand we can derive the self-consistency equation for N

$$\left\langle -\frac{\partial H_{MF}}{\partial(4N/g)} \right\rangle = \sum_r \left\langle \epsilon_r f_r^\dagger \frac{\sigma^z}{2} f_r \right\rangle = L^2 N, \quad (8)$$

where L is the linear system size. Using the spectral function of the lower band (we consider $T=0$) this gives

$$gN = \frac{N}{L^2} \sum_{\mathbf{k}} \frac{1}{\sqrt{(2N/g)^2 + \varepsilon(\mathbf{k})^2 + \Delta(\mathbf{k})^2}}. \quad (9)$$

This equation has a trivial solution $N=0$, but it is obvious from Eq. (7) that a nonzero solution, if it exists, has lower energy. So the system has two phases, achieved by tuning the value of g. The critical value g_c is given by

$$g_c = \frac{1}{L^2} \sum_{\mathbf{k}} \frac{1}{\sqrt{\varepsilon(\mathbf{k})^2 + \Delta(\mathbf{k})^2}}. \quad (10)$$

For $g > g_c$ there is no nonzero solution and so $N=0$. But for $g < g_c$ we have $N \neq 0$. From Eq. (9) we can also derive the behavior of N at critical point within the mean field:

$$N \propto \begin{cases} 0 & \text{for } g > g_c, \\ g_c - g & \text{for } g < g_c. \end{cases} \quad (11)$$

Note that in the magnetic phase the nonzero N induces a gap for the spinons.

To study low-energy properties, we will set up a continuum effective theory. In the next section we will include fluctuations in this continuum field theory. In the spin liquid state, the spectrum consists of two Fermi points, located at $k_x = k_y = \pi/2$ and $k_x = -k_y = -\pi/2$ [at these points $\varepsilon(\mathbf{k}) = \Delta(\mathbf{k}) = 0$], in the reduced Brillouin zone. There are gapless spinon excitations near these nodes with a Dirac-like linear dispersion. A low-energy description of the spin liquid is then possible in terms of a continuum field theory of massless Dirac spinons (a brief review that helps fix notation is in Appendix A). To study the magnetic transition described above within this continuum field theory, we need to introduce a "mean field" that couples to the (π, π) component of the physical spin density. The resulting action takes the form

$$S_m = \int d^2x \, d\tau \, \bar{\psi} \left(-i\gamma^\mu \partial_\mu + i\lambda \mu^z N \frac{\sigma^z}{2} \right) \psi. \quad (12)$$

In this representation, ψ consists of four two-component Dirac fields. The four Dirac fields arise from the presence of two physical spin species together with two pairs of nodes. The Pauli matrices $\vec{\sigma}$ act on the spin index while the $\vec{\mu}$ are Pauli matrices acting on the node index. It is readily seen that the combination $(i/2)\bar{\psi}\mu^z\vec{\sigma}\psi$ is precisely the continuum form of the physical spin density near (π, π). In the mean-field theory N is to be determined self-consistently. The coupling λ is proportional to coupling $1/g$ and from now on the momenta are considered with respect to the nodes. As expected a nonzero N gaps out the Dirac spinons. This gap vanishes upon approaching the phase transition to the spin liquid. The inverse of this gap determines a diverging length scale—within the mean-field theory this length scale describes the decay of the *connected* part of the spin correlations near (π, π). This may be seen by a direct calculation (described in Appendix C) which gives

$$e^{i\vec{Q}\cdot\vec{r}} \langle S_i(0) S_j(r) \rangle_c \propto \frac{e^{-r/\xi}}{r^4} \left(1 + \frac{r}{\xi} \right) \delta_{ij}. \quad (13)$$

So the connected correlation for $r \ll \xi$ is a power-law decaying function with fourth power of r. For $r \gg \xi$ it is an exponentially decaying function, with correlation length ξ and a prefactor which decays as the third power of r. The correlation length at the critical point diverges as

$$\xi \propto \frac{1}{|\lambda - \lambda_c|} \sim \frac{1}{|g - g_c|}. \quad (14)$$

III. BEYOND MEAN-FIELD THEORY

In this section we consider the effects of fluctuations beyond the mean-field theory described above. In the spin liquid phase far from the magnetic transition the crucial fluctuations are those associated with the phase of the spinon hopping parameter. These are to be thought of as gauge fluctuations associated with a (compact) U(1) gauge field that is coupled minimally to the spinons. Recent work has shown that the *d*RVB spin liquid is stable to such gauge fluctuations[23] (at least within a systematic large-N expansion where N is the number of Dirac spinons). Throughout this paper we will assume that this stability persists to the physically relevant case $N=4$. The low-energy theory of the resulting phase is described by massless QED in three space-time dimensions:

$$S = \int d^2x\, d\tau \{ -\bar{\psi}[i\gamma^\mu(\partial_\mu + iea_\mu)]\psi + (\epsilon_{\mu\nu\kappa}\partial_\nu a_\kappa)^2 \}. \tag{15}$$

Here a_μ is a fluctuating U(1) gauge field which may be taken to be noncompact at the low energies. This theory flows to a conformally invariant fixed point. Various physical quantities have nontrivial power-law correlations at the resultant spin liquid fixed point.[39] In particular the (π,π) spin correlator decays as a power law:

$$e^{i\vec{Q}\cdot\vec{r}}\langle \vec{S}(0)\cdot\vec{S}(r)\rangle \sim \frac{1}{r^{2\Delta}}. \tag{16}$$

The exponent Δ is not known—a rough estimate from projected wave functions[40,41] gives $\Delta \approx 0.75$. The dynamical spin correlations at (π,π) in the scaling limit follow straighforwardly from the relativistic invariance of the field theory above. For the full zero-temperature dynamical spin susceptibility, we have

$$\chi''_{SL}(q,\omega) \sim \frac{1}{\omega^{2-\eta}} F\left(\frac{\omega}{vq}\right). \tag{17}$$

Here $\vec{q}$ is the deviation of the wave vector from $\vec{Q}=(\pi,\pi)$, F is a universal scaling function, and v is a nonuniversal spinon velocity associated with the nodal Dirac dispersion. The exponent η is the anamolous dimension of the staggered spin and is related to Δ through $2\Delta = 1+\eta$. Due to the power law spin correlations, this spin liquid phase has been dubbed an "algebraic spin liquid."[39] Note that the spinons are not good quasiparticles at low energies in the spin liquid phase. Indeed there presumably is no quasiparticle description of the spectrum (rather like at interacting quantum critical points). Nevertheless the field theory above in terms of spinons provides a useful description of the system.

A remarkable feature of the *d*RVB algebraic spin liquid phase is the emergence of a huge global symmetry group characterizing the low-energy fixed point. The low-energy theory has an SU(4) symmetry corresponding to free unitary rotations between the four Dirac species. In addition the irrelevance of space-time monopoles at low energies implies a nontrivial global U(1) symmetry associated physically with the conservation of internal magnetic flux. Reference 30 studied a number of consequences of the SU(4) symmetry. In particular it showed that several other competing order parameters had the same power-law correlators as the Néel vector -these include the order parameter associated with the columnar or plaquette VBS orders.

Near the transition to the antiferromagnetic state, we must treat the Néel field introduced in the previous section as a fluctuating vector $\vec{N}$. Further upon integrating out high energy spinons (i.e. ones far away from the nodes), this $\vec{N}$ field will develop some dynamics of its own. The resulting action takes the form

$$S = \int d^2x\, d\tau \Bigg(-\bar{\psi}[i\gamma^\mu(\partial_\mu + iea_\mu)]\psi + i\lambda\bar{\psi}\left(\mu^z \vec{N}\cdot\frac{\vec{\sigma}}{2}\right)\psi + (\epsilon_{\mu\nu\kappa}\partial_\nu a_\kappa)^2 + \frac{(\partial_\mu \vec{N})^2}{2} + r\frac{(\vec{N})^2}{2} + \frac{u}{4!}[(\vec{N})^2]^2 \Bigg). \tag{18}$$

In writing this action we have ignored anisotropies in the spinon velocities at the Dirac node and any difference between the velocities of spinon and N fields. Later we will show that all of these velocity anisotropies are irrelevant (if small) at the critical fixed point between the *d*RVB ASL and Néel states (see Appendix C 5).

In the presence of the coupling to the $\vec{N}$ field, the action no longer has full SU(4) global symmetry. An SU(2) subgroup—corresponding to physical spin rotations—is still obviously a symmetry. This involves an SU(2) spin rotation of the ψ field together with an O(3) rotation of the $\vec{N}$ vector. In addition, the global transformation

$$\psi \to e^{i\theta\mu^z}\psi \tag{19}$$

with θ a constant is also a symmetry. This is a U(1) subgroup of the full SU(4) symmetry. Thus the action has a global $SU(2)\times U(1)$ symmetry apart from the $U_{flux}(1)$ associated with the gauge flux conservation. The extra U(1) symmetry that survives from the full SU(4) has the consequence that fermion bilinears such as $\bar{\psi}\mu_x\psi, \bar{\psi}\mu_y\psi$ can be freely rotated into another. In the original spin model, these operators transform identically to the VBS order parameter. The U(1) symmetry then implies that the columnar and plaquette order parameters can be rotated into one another, and hence will have identical correlations.

Let us now study some general aspects of the two phases, near the phase transition.

A. Precursor fluctuations in the spin liquid

We will first consider the precursor fluctuations of the magnetic ordering in the spin liquid side.

First consider the limit $\lambda=0$. Then the $\vec{N}$ field decouples from the spinon gauge sector. It is instructive to think about the spectral function for the (π,π) spin correlations in the spin liquid phase in this limit. It is simply a sum of two pieces as shown in Fig. 4—a diverging power law coming from the ASL, and a sharp δ function peak coming from the N fluctuations. Now consider turning on a small nonzero λ. The low-frequency divergence of the spin susceptibility will

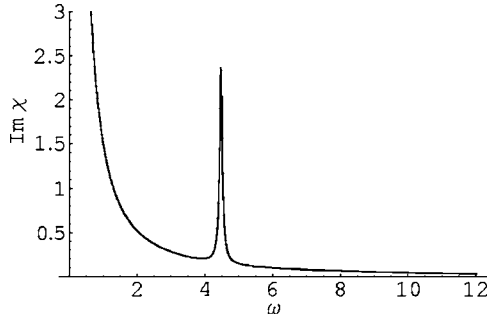

FIG. 4. Dynamical spin susceptibility at (π,π) in the spin liquid phase in the $\lambda=0$ limit.

be unaffected by the coupling to the fluctuating $\vec{N}$ field (this follows from the assumed stability of the ASL fixed point). However, the δ function peak coming from the $\vec{N}$ field will now be broadened due to decay into two spinons. The broadening may be described within a simple random-phase approximation (RPA) (for details see Appendix B).

In Fig. 5 we plot the dynamical spin susceptibility at (π,π) as the phase transition is approached (by decreasing r). Note that as expected, the peak coming from the $\vec{N}$ fluctuations "softens" on approaching the transition.

B. Magnetic state

When the parameter r is sufficiently negative the $\vec{N}$ field will condense leading to magnetic long-range order. In the continuum field theory this may be viewed as a spin density wave state that arises out of the *d*RVB ASL. In this subsection we will argue that contrary to naive expectations, it is in fact a different state from a conventional Néel state—rather it is a fractionalized antiferromagnet in the same spirit as that studied in Refs. 22 and 33. This apparent problem will be cured once we include the effects of monopole fluctuations (ignored so far). We will show that this fractionalized antiferromagnet evolves at long length and time scales into the conventional Néel antiferromagnet.

Consider first the description of the Néel ordered state within the mean field theory developed in Sec. II. The mean-field spectrum consists of *gapped* spin-1/2 spinons.[51] It is important to realize that the spinons are merely gapped—however, they have not disappeared from the spectrum. Now consider including fluctuations as in Sec. III. The important fluctuations are those associated with slow rotation of the direction of the Néel order parameter $\vec{N}$ (spin waves) and those asociated with the phase of the fermion hopping T (gauge fluctuations). These are both conveniently discussed within the continuum theory in Eq. (19), which obtains close to the critical point. Integrating out the gapped spinons, we may obtain an effective action for the spin waves and the gauge fluctuations. To quadratic order in both the transverse component of the Néel vector $\vec{N}_\perp$ and the gauge field a, we get

$$S_{eff}=\int d^3x\frac{\rho_s}{2}(\partial_\mu\vec{N}_\perp)^2+\frac{g}{2}(\epsilon_{\mu\nu\kappa}\partial_\nu a_\kappa)^2+\cdots, \qquad (20)$$

where the ellipsis refers to higher-order terms that are unimportant at low energies. The first term describes the expected

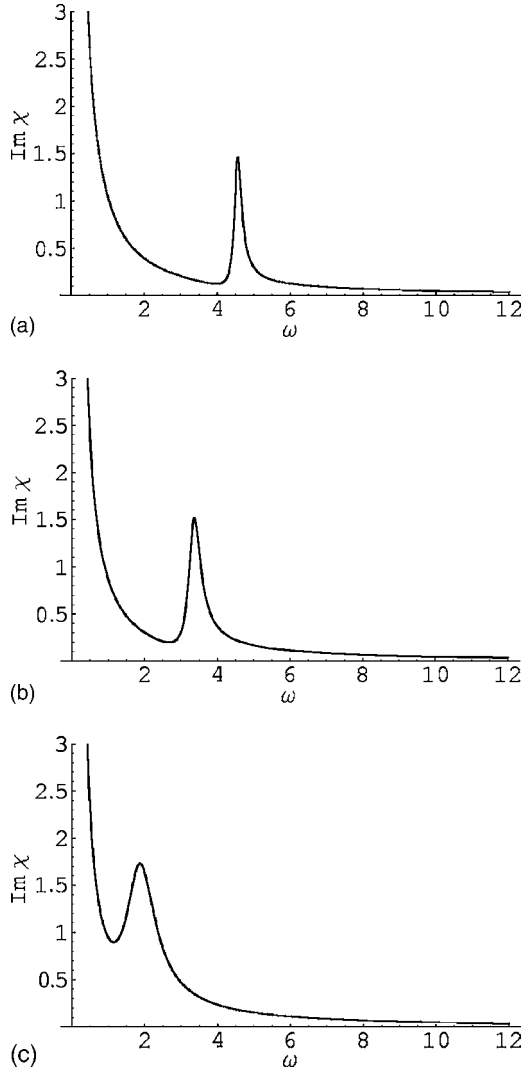

FIG. 5. Dynamical spin susceptibility at (π,π) after turning on a nonzero value for λ. The plot shows the change upon approaching the transition from (a) to (c). Note the softening of the $\vec{N}$ peak, as the transition occurs.

gapless spin wave excitations. The second term describes a gapless linear dispersing photon associated with the gauge fluctuations. This extra gapless mode provides a sharp low-energy distinction between this Néel state (as described so far) and the conventional one. The gapless photon mode is minimally coupled to the gapped spinons—the presence of gapped spinons serves as another distinction from the conventional Néel state. Thus the antiferromagnet state is to be characterized as a "fractionalized antiferromagnet" with a U(1) gauge structure. Following the notation of Ref. 33, we will dub it a U(1) AF*.

Let us now include monopole fluctuations. In this magneticaly ordered phase, the low-energy gauge action is that of free Maxwell theory in 2+1 dimensions. Then standard arguments show that the monopoles are strongly *relevant*. Thus the U(1) AF* state (in two dimensions) is ultimately unstable to monopole proliferation. The result is to gap out the photon mode and cause confinement of all objects that carry nonzero gauge charge. In particular it implies that the spinons (which

survived as gapped excitations when monopoles are ignored) will now be confined and disappear from the spectrum. The resulting state is thus simply smoothly connected to the conventional Néel state. Thus including monopole fluctuations cause an instability of the unconventional U(1) AF* state toward the conventional Néel state.

C. Projected wave functions

Before continuing we digress briefly to make contact with the large body of work on Gutzwiller-projected superconducting wave functions (see Ref. 41 and references therein), as a route to implementing RVB ideas. Of interest to us will be studies on projected d-wave BCS states and their variants. In the slave particle description, a useful guess for a prototypical wave function for a state is obtained by taking the mean-field state and projecting it onto the space of physical states. At half filling this is equivalent to doing a Gutzwiller projection on the mean-field state. According to this prescription, a guess for the wave function of the dRVB algebraic spin liquid will simply be

$$|d\mathrm{RVB}\rangle = P_G|d\mathrm{BCS}\rangle, \tag{21}$$

where $|d\mathrm{BCS}\rangle$ is the mean-field ground state of a d-wave superconductor at half filling with just nearest neighbor hopping and pairing on the square lattice. Correspondingly, a guess for the wave function of the magnetic state, as we have obtained it, would simply be

$$|\mathrm{AF}\rangle = P_G|d\mathrm{BCS} + \mathrm{SDW}\rangle, \tag{22}$$

where SDW indicates the spin density wave. The preprojected state on the right simply has spin density wave order at (π,π) coexisting with the d-wave superconductivity. Such wavefunctions have been studied numerically[42] and are known to have excellent energy for the nearest neighbor Heisenberg model. From our considerations in the previous section, we would expect that this wave function is a prototype for a *confined* antiferromagnet with no finite energy spinons. Some support for this expectation comes from the work of Ref. 43 which studied the properties of a single hole in that state. The quasiparticle residue was found to be nonzero, consistent with that expected in a confined antiferromagnet.

IV. PHASE TRANSITION: GENERALITIES

Let us now consider the phase transition between the dRVB ASL and the Néel state. In the limit $\lambda=0$, the $\vec{N}$ vector fluctuations are decoupled from the ASL and the magnetic transition is simply in the universality class of the usual O(3) fixed point in $D=3$ space-time dimensions. Note that in this limit mean-field theory predicts that the Néel order parameter vanishes with exponent $\beta=1/2$ on approaching the transition. What is the effect of turning on a weak λ at this decoupled transition? First note that in the mean-field theory of Sec. II we found that the Néel order parameter vanished with exponent $\beta=1$ clearly different from the $\lambda=0$ limit. Thus a nonzero λ already changes the answers within mean-field theory. More generally the effects of a weak λ may be assessed by considering the renormalization group flow of λ at the decoupled fixed point. We have

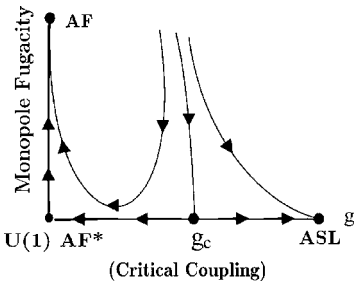

FIG. 6. Renormalization flow diagram near the critical fixed point. The vertical axis is the monopole fugacity; the horizontal axis is a coupling g which describes the strength of the short-range part of the spinon interaction.

$$\frac{d\lambda}{dl} = (D - \Delta_N - \Delta)\lambda, \tag{23}$$

where $D=3$ is the space-time dimension, Δ_N is the scaling dimension of the N field at the $D=3$ O(3) fixed point, and Δ is the scaling dimension of the spin operator near (π,π) at the dRVB ASL fixed point. Here l is the usual logarithmic renormalization scale. We have $\Delta_N=(1+\eta_N)/2\approx 1/2$, and $\Delta=(1+\eta)/2$. Thus $D-\Delta_N-\Delta\approx 2-\eta/2$. With the rough estimate $\eta\approx 0.5$, we find that λ is strongly relevant at the decoupled fixed point. Thus the true critical behavior will involve strong coupling between the $\vec{N}$ field and the spinons of the ASL. In Sec. V, we will study this critical behavior in a controlled $3-\epsilon$ dimension. A very similar field theory where a fluctuating O(3) vector field was coupled to massless Dirac fermions was studied many years ago by Balents *et al.*[44] in a different physical context. The main difference between the theory of Balents *et al.* and the action in Eq. (18) is the presence of the gapless gauge fields in the latter. We will see that this modifies the universality class of the transition from that in Ref. 44.

What about monopole fluctuations at this critical point? Let us first review the situation in the paramagnetic algebraic spin liquid state. Recent work has argued[23] that when the number of Dirac species N is sufficiently large (i.e., bigger than some N_c) the monopoles are formally irrelevant at the ASL fixed point.[52] In the large-N expansion, the monopole scaling dimension will be $o(N)$ both at the ASL fixed point and at the critical fixed point—thus at least for large enough N the monopoles are irrelevant at the critical fixed point as well. In this paper we will make the crucial assumption that this irrelevance continues to hold at $N=4$, i.e., for SU(2) spin models (see Fig. 6).

With this assumption the monopole fugacity is irrelevant at the critical fixed point (and the paramagnetic ASL fixed point) but relevant at the ordered fixed point of the continuum field theory in Eq. (18). In renormalization group language, the monopole fugacity is a dangerously irrelevant coupling. The length scale ξ_m at which the photon gets gapped (which may loosely be dubbed the "confinement scale") in the magnetic side may be estimated as follows. Let

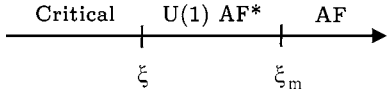

FIG. 7. Crossover length scales in the magnetic state close to the transition to the spin liquid. The shorter length scale ξ describes the crossover from the critical state to the fractionalized antiferromagnet. The longer scale ξ_m is where this exotic antiferromagnet crosses over to the conventional Néel state through confinement. Both scales diverge near the critical point but ξ_m diverges faster than ξ.

the monopole scaling dimension at the critical point be $\Delta_m > 3$. Upon scaling out of the critical region in the ordered state to the correlation length scale ξ, the monopole fugacity will renormalize to $z_\xi \sim \xi^{3-\Delta_m}$. It is beyond this scale ξ that the action in Eq. (20) starts applying. In the free Maxwell theory that obtains beyond ξ, the monopole fugacity grows. A standard matching argument now gives $\xi_m \sim \xi^{(\Delta_m-1)/2}$. Thus ξ_m diverges faster than ξ. The physics on scales $\xi \ll L \ll \xi_m$ is that of the fractionalized antiferromagnet U(1) AF*. It is only at the longest scales $L \gg \xi_m$ that the conventional Néel behavior is obtained (Fig. 7).

V. ϵ EXPANSION FOR CRITICAL PROPERTIES

In this section we will show how the structure of the critical fixed point can be studied in a formal expansion near three space dimensions. Some care is necessary in dealing with the Dirac matrices in arbitrary dimension. But here, following Ref. 44, we will sidestep this issue. We will perform calculations in a perturbative expansion of the coupling constants in $d=2$, take the traces over the Dirac matrices, and then finally, in evaluating momentum integrals, set $d=3-\epsilon$. As a warmup we first describe the ASL fixed point within this ϵ expansion.

A. ASL in the ϵ expansion

Before starting the ϵ expansion studies for the full theory, we study the ASL phase with this approach. To do that we consider action (18) and assume $N=0$. Then it reduces to the usual QED_3 action. The flow equation for this theory is well known[45] (and also calculated in Appendix C):

$$\beta_{e^2} = \epsilon e^2 - \frac{16}{3}\frac{e^4}{(4\pi)^2}. \tag{24}$$

Here $\epsilon=3-d$. This flow equation indicates the presence of a nontrivial fixed point of order ϵ at

$$e^{*2} = 3\pi^2\epsilon. \tag{25}$$

This is the pure ASL fixed point. The microscopic derivation of the continuum field theory for the spin liquid allows for a velocity anisotropy between the two spinon nodes. This anisotropy was found to be irrelevant in the large-N limit of QED_3.[30,46–48] Here we examine its fate within the ϵ expansion. Direct calculation (Appendix C 5) shows that $\beta_\delta = -\delta[14/3(4\pi)^2]e^{*2} = -\frac{7}{8}\delta\epsilon$, where δ measures the velocity anisotropy (i.e., $\delta=0$ corresponds to isotropic QED_3), so that it is irrelevant at $o(\epsilon)$. Combined with the large-N result, this is strong evidence for its irrelevance at the physically relevant ASL fixed point for $N=4$ in two space dimensions. As noted in previous papers[30] this irrelevance implies that the $N=4$ ASL fixed point has global SU(4) symmetry corresponding to free unitary rotation between the four Dirac species.

Finally we can examine the scaling of gauge neutral fermion bilinears (such as the Néel vector) in the ϵ expansion. This is conveniently done by adding a source term that couples to such a bilinear, and calculating the one-loop correction to the corresponding vertex (see Appendix C). We find that the (π,π) component of the spin has scaling dimension $\Delta = 3 - 1.94\epsilon$. Setting $\epsilon=1$ gives the estimate $\Delta \approx 1.06$. This implies extremely slow decay of the corresponding correlator. This estimate may be compared with that from the $1/N$ expansion directly in $d=2$ which gives $\Delta \approx 1.54$. Thus both expansions give slow decay for the Néel correlations that are strongly enhanced compared to the mean-field results.

B. Critical fixed point

In this section we study the critical point within the ϵ expansion by including the fluctuating $\vec{N}$ field. From the action (18) we have three types of vertices and 11 different one-loop diagrams. At one-loop level, as derived in Appendix C, we get the following set of flow equations:

$$\beta_{e^2} = \epsilon e^2 - \frac{16}{3}\frac{e^4}{(4\pi)^2}, \tag{26}$$

$$\beta_{\lambda^2} = \epsilon\lambda^2 - \frac{10}{(4\pi)^2}\lambda^4 + \frac{10}{(4\pi)^2}e^2\lambda^2, \tag{27}$$

$$\beta_u = \epsilon u - \frac{11}{3}\frac{u^2}{(4\pi)^2} - 16\frac{\lambda^2 u}{(4\pi)^2} + 96\frac{\lambda^4}{(4\pi)^2}, \tag{28}$$

$$\beta_r = \left(2 - \frac{5}{3}\frac{u}{(4\pi)^2} - 8\frac{\lambda^2}{(4\pi)^2}\right)r. \tag{29}$$

Note that the flow equation for electric charge is the same as the usual quantum electrodynamics. In fact, gauge invariance dictates this form[45,49] (to keep the form ea_μ invariant under renormalization group (RG) flow we need to have $Z_e/\sqrt{Z_a} = 1$). From these we can get the following fixed points:

$$e^{*2} = 0, \tag{30}$$

$$\lambda^{*2} = \frac{8\pi^2}{5}\epsilon, \tag{31}$$

$$u^* = \frac{384\pi^2}{55}\epsilon. \tag{32}$$

This fixed point describes the transition in the absence of the gauge field and was first discussed by Balents *et al.*[44] Our calculations at this fixed point matches this previous work which therefore provides a useful check. As another check at

this fixed point, if we consider our theory, with the three-component $\vec{N}$ field replaced by a scalar field ϕ, it represent a Yukawa-like theory, which has been studied in Ref. 45. Our results then can be partially checked against these previous calculations. The full flow equations admit another fixed point located at

$$e^{*2} = 3\pi^2\epsilon, \tag{33}$$

$$\lambda^{*2} = \frac{23\pi^2}{5}\epsilon, \tag{34}$$

$$u^* = \frac{12\pi^2}{55}(-36 + \sqrt{12934})\epsilon. \tag{35}$$

It is readily checked that the $e^2=0$ fixed point is unstable toward this one. Thus the presence of the gauge field has changed the universality class of the transition. Here we should also note that at the one-loop level, the calculation in Appendix C 5 shows that at this fixed point, the velocity anisotropy is irrelevant at $o(\epsilon)$. So this fixed point is also stable against small velocity anisotropy. Now using the flow equation for r [Eq. (29)], it is easy to extract the exponent ν for this fixed point:

$$\frac{1}{\nu} = 2 - 4.07\epsilon. \tag{36}$$

Note that simply setting $\epsilon=1$ gives an unphysical answer. This is a signal that the leading order ϵ expansion is not quantitatively very accurate in estimating scaling dimensions in two space dimensions. Despite this the ϵ expansion is useful to describe the structure of the fixed points and the trends of the various exponents.

It is very interesting to ask about the behavior of the staggered spin correlations [i.e., near (π,π)] at this critical point. Naively there are two different physical operators that have the same symmetries as the staggered spin: the vector $\vec{N}$ and the fermion bilinear $\vec{N}_A^z = \bar{\psi}\mu_z\vec{\sigma}\psi$. Thus in writing down an expression for the staggered spin in terms of the fields of the continuum theory, we must include both contributions:

$$e^{i\vec{Q}\cdot\vec{x}}\vec{S}(\vec{x}) \sim c_1\vec{N} + c_2\vec{N}_A^z + \cdots. \tag{37}$$

The ellipsis refers to other operators with larger scaling dimension that also have the same symmetries as the staggered spin. The coefficients $c_{1,2}$ are nonuniversal. Now consider the scaling of the staggered spin. If $\lambda=0$, then the fermion bilinear and $\vec{N}$ scale independently. Near $d=3$, and with the available estimate of the scaling dimension of the fermion bilinear at the ASL, it is readily checked that $\vec{N}$ has the lower scaling dimension. Hence the long-distance decay of the staggered spin correlations will be determined by $\vec{N}$ in the $\lambda=0$ limit. What happens when λ is nonzero as at the nontrivial fixed point above in the ϵ expansion? It is expected that the true scaling fields will be some linear combinations of $\vec{N}$ and $\vec{N}_A^z$ which will have the form

$$\vec{\phi}_1 \sim A_1\vec{N} + A_2\vec{N}_A^z, \tag{38}$$

TABLE I. List of observables in the spin model that are symmetry equivalent to the N^a and M fermion bilinears. For some of these we label the sites around the plaquette with lower left corner at $\vec{r}$ by the numbers 1,…,4. Precisely, $\vec{S}_1=\vec{S}_{\vec{r}}$, $\vec{S}_2=\vec{S}_{\vec{r}+\vec{x}}$, $\vec{S}_3=\vec{S}_{\vec{r}+\vec{x}+\vec{y}}$, and $\vec{S}_4=\vec{S}_{\vec{r}+\vec{y}}$.

Field theory	Spin model	Scaling dimension
$\vec{N}_A^x, \vec{N}_A^y$	$(-1)^{r_x+1}\vec{S}_{\vec{r}}\times\vec{S}_{\vec{r}+\vec{y}}, (-1)^{r_y}\vec{S}_{\vec{r}}\times\vec{S}_{\vec{r}+\vec{x}}$	$3-0.5\epsilon$
$\vec{N}_A^z$	$(-1)^{r_x+r_y}\vec{S}_{\vec{r}}$	$3-1.65\epsilon$
$\vec{N}_B$	$(-1)^{r_x+r_y}[(\vec{S}_1+\vec{S}_3)(\vec{S}_2\cdot\vec{S}_4) + (\vec{S}_2+\vec{S}_4)(\vec{S}_1\cdot\vec{S}_3)]$	$3-1.65\epsilon$
N_C^x, N_C^y	$(-1)^{r_y}\vec{S}_{\vec{r}}\cdot\vec{S}_{\vec{r}+\vec{y}}, (-1)^{r_x}\vec{S}_{\vec{r}}\cdot\vec{S}_{\vec{r}+\vec{x}}$	$3-2.8\epsilon$
N_C^z	$[\vec{S}_1\cdot(\vec{S}_2\times\vec{S}_4) - \vec{S}_2\cdot(\vec{S}_3\times\vec{S}_1) + \vec{S}_3\cdot(\vec{S}_4\times\vec{S}_2) - \vec{S}_4\cdot(\vec{S}_1\times\vec{S}_3)]$	$3+0.65\epsilon$
M	$[\vec{S}_1\cdot(\vec{S}_2\times\vec{S}_4) + \vec{S}_2\cdot(\vec{S}_3\times\vec{S}_1) + \vec{S}_3\cdot(\vec{S}_4\times\vec{S}_2) + \vec{S}_4\cdot(\vec{S}_1\times\vec{S}_3)]$	$3+0.65\epsilon$

$$\vec{\phi}_2 \sim B_1\vec{N} + B_2\vec{N}_A^z. \tag{39}$$

These fields will have scaling dimension $\Delta_{1,2}$ with (by definition) $\Delta_1<\Delta_2$ so that the long-distance decay will be dominated by $\vec{\phi}_1$. The coefficients $A_{1,2}$ and $B_{1,2}$ will be determined by the fixed point theory. At $o(\epsilon)$ we expect $A_1 \sim o(1), A_2 \sim o(\epsilon), B_1 \sim o(\epsilon), B_2 \sim o(1)$. Thus to obtain the scaling dimensions $\Delta_{1,2}$ to $o(\epsilon)$ we can ignore the "mixing" terms A_2, B_1, and simply calculate the anamolous dimension of $\vec{N}$ and $\vec{N}_A^z$.

The exponent η for the N field (which determines the scaling dimension) is easily calculated from the field renormalization coefficient Z_N:

$$Z_N = 1 - \frac{8}{(4\pi)^2}\frac{\lambda^2}{\epsilon}. \tag{40}$$

η is then given by the coefficient of $1/\epsilon$ in Z_N:

$$\eta = 2.3\epsilon \tag{41}$$

so that $\Delta_1 = 1 + 0.65\epsilon$. The dimension Δ_2 is readily calculated as in our discussion of the ASL above. We find $\Delta_2 = 3 - 1.65\epsilon$.

It is straightforward to determine the scaling dimension of all the fermion bilinears related to $\vec{N}_A^z$ by SU(4) rotations. These are listed in Table I; the corresponding Feynman diagrams are in Appendix C. The absence of SU(4) symmetry at the critical fixed point implies that these bilinears mostly have different scaling dimensions. Some weak constraints follows from the U(1) subgroup of the SU(4) that remains unbroken. For instance it implies that N_A^x, N_A^y have the same scaling dimension. As emphasized before physically this implies identical scaling of the plaquette and columnar VBS order parameters at this critical point.

Here we have defined the observable as

$$\vec{N}_A{}^i = -i\bar{\psi}\mu^i\vec{\sigma}\psi, \tag{42}$$

$$\vec{N}_B = -i\bar{\psi}\vec{\sigma}\psi, \tag{43}$$

$$N_C{}^i = -i\bar{\psi}\mu^i\psi, \tag{44}$$

$$M = -i\bar{\psi}\psi. \tag{45}$$

We see that $\vec{N}_A{}^z$ corresponds to the Néel vector and $iN_c^x + N_c^y$ corresponds to the VBS order parameter.

C. Discussion

Now let us examine the trends shown by the exponents calculated in Table I. Note that the scaling dimensions of these gauge-invariant bilinears are the same in the ASL phase due to the SU(4) symmetry. So for all of them we have $\Delta = 3 - 1.94\epsilon$. Remarkably the scaling dimension of the VBS order parameter (N_C^x, N_C^y) is *smaller* at the critical point than it is in the ASL phase. Thus the VBS fluctuations are *enhanced* by the critical $\vec{N}$ vector fluctuations. All other fermion bilinears decay faster at the critical point as their scaling dimension is increased. This includes the vector $\vec{N}_A{}^z$ which is the contribution from the gapless fermions to the Néel vector. It is at present not clear whether in $d=2$ the susceptibilities of these other operators (such as $\vec{N}_A^x$, etc.) will diverge at the critical point (though they apparently do in the ASL phase). In contrast the VBS susceptibility will presumably diverge at the critical point. The divergence will be faster at the critical point (as say a function of temperature) than in the ASL phase. On the magnetic side the VBS susceptibility will of course be finite in the ground state. However it will diverge as the transition is approached and will thus be large if the antiferromagnet is to be regarded as being close to this critical point. Thus a qualitative conclusion from our calculations is that in the limit that the Néel state can be usefully regarded as being created out of the *d*RVB spin liquid, it will also have enhanced VBS susceptibility.

The diverging VBS susceptibility also provides an interesting way to define the correlation length ξ in terms of directly measurable quantities. Consider the VBS corelations in the magnetic side as a function of length scale. At scales smaller than ξ they will decay as a power law. However at scales larger than a length set by ξ, they will decay exponentially. Thus ξ may be usefully defined as the correlation length for VBS fluctuations in the ordered antiferromagnet.

VI. IMPLICATIONS FOR CUPRATE THEORY

We now discuss some of the implications of our results for theories of the cuprates. As we emphasized in the Introduction, a second-order transition between a collinear Néel state and a gapless spin liquid is attractive for a number of reasons. Here we explore this in somewhat greater detail. We will obtain a qualitative understanding of neutron resonance but do not attempt a quantitatively accurate calculation. Our thinking on the cuprates is guided by Fig. 1. We suppose that increasing magnetic frustration (the parameter g) at zero doping can induce a transition out of the collinear Néel state to a spin liquid. Theoretically the spin liquid is expected to evolve rather naturally into a superconductor when it is doped. The real material starts off in the antiferromagnetic state at zero doping. The idea is that doping (apart from introducing holes) also has the effect of increasing g. Then we can hope that the intermediate- and long-scale physics of the resulting doped superconductor may be fruitfully described as a doped spin liquid. This is the rationale behind the spin-liquid-based approach to the cuprates.

With this point of view in mind let us consider the effects of doping the *d*RVB algebraic spin liquid phase discussed in this paper. Previous papers (for a review see Ref. 50) have shown how a *d*-wave superconductor (*d*SC) with gapless nodal quasiparticles emerges quite naturally upon doping this spin liquid. Now consider reducing the doping in the real material. According to Fig. 1 this also has the effect of reducing the magnetic frustration g. This pushes the "parent" spin liquid state closer to the transition to antiferromagnetism. The magnetic response of the parent spin liquid at wave vector (π, π) then evolves in the manner shown in Fig. 5. Note in particular that if the transition to the magnetic state is second order then the "resonance" due to the $\vec{N}$ fluctuations softens. How does this impact the magnetic response in the doped superconductor?

The doping of the spin liquid is incorporated theoretically by the introduction of two species of charged spinless bosons b_1 and b_2. These bosons also carry gauge charges $+1$ and -1, respectively. Superconductivity is achieved when both b_1 and b_2 condense with equal amplitude. This route from the *d*RVB spin liquid to the *d*SC has two important features. First the gauge charge carried by the bosons implies that the gapless gauge fluctuations of the spin liquid are quenched in the superconducting state (by the Anderson-Higgs mechanism). The spinons evolve naturally into the fermionic quasiparticle excitations of the *d*SC. The nodal structure of the spinons is retained—however, coupling between the b and f fields moves the nodes of the quasiparticles away from $(\pi/2, \pi/2)$ by an amount proportional to the doping x.

For the magnetic response this has some crucial implications. First, when compared with Fig. 5, the diverging low-frequency response is destroyed as it comes entirely due to the gapless gauge fluctuations of the spin liquid. The resonance due to the triplon $\vec{N}$ mode then becomes the most prominent feature in the (π, π) response. Further, its frequency will soften as the doping is reduced. Second, as the fermionic quasiparticles no longer have nodes at (π, π) they only weakly damp out this reonance. Finally, the fermionic quasiparticles will still contribute some background magnetic response which can now be usefully addressed in a standard RPA calculation. Such calculations have been reported before in the literature, and give rise to incommensurate continuum scattering at frequencies below the resonance that appear to be consistent with experiment.

Since the original discovery of the neutron resonance peak, there have been two more or less independent interpretations. One view is to describe it as a soft mode associated with the magnetism of the undoped Mott insulator. This view has the advantage that it provides a natural explanation of the softening of the resonance frequency with underdoping. The other view has been to simply regard it as an $S=1$ collective

mode of weakly correlated fermionic quasiparticles in the superconducting state. The description given above unifies these two different interpretations. Indeed in the parent spin liquid the triplon $\vec{N}$ mode may be viewed as a particle-hole triplet exciton made out of *spinons*—rather than electrons. This mode appears naturally as a recognizable peak in the magnetic response upon approaching the AF state. Doping this spin liquid then leads to a superconductor with gapless fermionic quasiparticles and a sharp gapped $S=1$ triplon.

VII. CONCLUSION

In this paper we have reconsidered the issue of possible second-order phase transitions out of the collinear Néel state into paramagnetic spin liquid states in two-dimensional quantum antiferromagnets. The particular spin liquid we considered is a *d*RVB state which has gapless spin excitations. Correspondingly there are nontrivial power-law correlations in the spin and other quantities. A useful description is provided in terms of gapless Dirac-like spinons that are coupled to a fluctuating U(1) gauge field. However, there is possibly no true quasiparticle description of the spectrum. Indeed this state is in a critical phase that is the two-dimensional analog of the one-dimensional spin-1/2 chain. In contrast to other simpler spin liquids which have a spin gap, a direct second-order transition to the collinear Néel state appears to be possible for such a two-dimensional algebraic spin liquid. We developed in some detail a theory for such a transition. Magnetic long-range order was obtained as a spin density wave transition of spinons. We argued that gauge fluctuations convert the resulting magnetic state into a conventional one that is smoothly connected to the usual Néel state. Thus the spinons disappear from the spectrum in the magnetic state. The theory for the transition shares a number of similarities with the deconfined critical points studied recently. Most importantly, there are two diverging length and time scales as the transition is approached from the magnetic side. The shorter of the two scales is associated with the onset of magnetic order from a critical soup of spinons. The second longer scale is associated with confinement of the spinons. It is in the intermediate length and time scale regime (i.e., between the two diverging lengths) that the magnetic ordering is correctly described as a spin density wave formed out of spinons. This intermediate-scale regime may also be characterized as a fractionalized antiferromagnet.

We noted several implications of our results for theories of the cuprates that regard them as doped spin liquids. First it allows us to develop a qualitative picture of the resonance mode seen in neutron experiments. Our picture unifies the existing descripions as a soft mode associated with the magnetic ordering in the insulator and as a triplet excition formed from a particle-hole pair of fermionic BCS quasiparticles. Indeed, in our description the resonance is a soft mode of the magnetic ordering that is formed as a particle-hole triplet exciton of spinons. This picture is closest to that in Ref. 20.

We have shown how magnetism may be incorporated into the spin-liquid-based approach to the cuprates. Central to this is the description of magnetism as a spin density wave ordering of spinons. Such a description has been explored before in a number of publications. As summarized in the first paragraph of this section, our work clarifies the range of validity of such a description. Indeed, should experiments reveal clear signatures for a fermionic spinon description of the intermediate-scale spin physics of the undoped cuprates then we could take that to be a signature of proximity to the quantum transition to the *d*RVB algebraic spin liquid.

ACKNOWLEDGMENTS

We thank Patrick Lee, M. Hermele, and X.-G. Wen for useful discussions. This work was supported by NSF Grant No. DMR-0308945. T.S. also acknowledges funding from the NEC Corporation, the Alfred P. Sloan Foundation, and an award from The Research Corporation.

APPENDIX A: DIRAC ACTION

Here we show that low-energy effective action is described by a continuum theory of fermionc spinons with Dirac dispersion. As mentioned before, we need to expand the Hamiltonian close to nodes at $(\pi/2,\pi/2)$ and $(-\pi/2,\pi/2)$. From now on (k_x,k_y) refer to deviation from the $(\pi/2,\pi/2)$ or $(-\pi/2,\pi/2)$ points. Here we explicitly derive the Hamiltonian near $(\pi/2,\pi/2)$. The other node is similar:

$$H=\begin{bmatrix} -\frac{4}{g}\vec{N}\cdot\frac{\vec{\sigma}}{2} & 2tk_+ - 2i\Delta k_- \\ 2tk_+ + 2i\Delta k_- & \frac{4}{g}\vec{N}\cdot\frac{\vec{\sigma}}{2} \end{bmatrix}, \tag{A1}$$

where $k_+=k_x+k_y$ and $k_-=k_x-k_y$. This Hamiltonian could be written in terms of 2×2 Pauli matrices which are defined as

$$\tau^x=\begin{bmatrix}0&1\\1&0\end{bmatrix},\quad \tau^y=\begin{bmatrix}0&-i\\i&0\end{bmatrix},\quad \tau^z=\begin{bmatrix}1&0\\0&-1\end{bmatrix}.$$

Using this notation and also adding the contribution from the $(-\pi/2,\pi/2)$ node we get the following form for the low-energy Hamiltonian:

$$H=\sum_{k_+,k_-} c_1^\dagger\left(2tk_+\tau^x+2\Delta k_-\tau^y-\frac{4}{g}\tau^z\vec{N}\cdot\frac{\vec{\sigma}}{2}\right)c_1 - c_2^\dagger\left(2tk_-\tau^x+2\Delta k_+\tau^y+\frac{4}{g}\tau^z\vec{N}\cdot\frac{\vec{\sigma}}{2}\right)c_2. \tag{A2}$$

Here c_1 and c_2 refer to $(\pi/2,\pi/2)$ and $(-\pi/2,\pi/2)$ nodes, respectively. They are two-component fermionic operators, each component representing one of the sites in the unit cell. The τ^i matrices operate in the space of these two components. Each component has an SU(2) spin index, where the σ matrices operate. Now assume $t=\Delta$ (i.e., ignore the velocity anisotropy which is irrelevant in renormaliztion group language) and we rename k_+ as k_y and k_- as k_x. Then introduce the new fermionic operators

$$\psi_1=-i\tau^x c_1, \tag{A3}$$

$$\psi_2=e^{i(\pi/4)\tau^z}c_2, \tag{A4}$$

and subsequently

$$\bar{\psi}_{1,2} = \psi^{\dagger}_{1,2}(i\tau^z). \tag{A5}$$

With these new variables, the Hamiltonian (A2) takes the following simple form:

$$H = \sum_{k_x,k_y} \bar{\psi}_1 \left(k_x \tau^x + k_y \tau^y + J\vec{N}\cdot\frac{\vec{\sigma}}{2} \right)\psi_1 + \bar{\psi}_2 \left(k_x \tau^x + k_y \tau^y - J\vec{N}\cdot\frac{\vec{\sigma}}{2} \right)\psi_2. \tag{A6}$$

Then using μ matrices that operate in the space made by the presence of two different nodes, we can put the node contributions (ψ_1 and ψ_2) as a single vector ψ. Then the Hamiltonian takes the form

$$H = \sum_{k_x,k_y} \bar{\psi} \left(k_x \tau^x + k_y \tau^y + iJ\mu^z \vec{N}\cdot\frac{\vec{\sigma}}{2} \right)\psi. \tag{A7}$$

This form in the continuum limit and in real space leads to the action given in Eq. (12).

APPENDIX B: RANDOM PHASE CALCULATION

We start with the partition function with an external magnetic field h that couples to the Neel vector:

$$Z = \int [D\psi][D\bar{\psi}][Da][DN] e^{-S}, \tag{B1}$$

$$S = S_N + S_{\psi,a} + S_{mixing} + S_h, \tag{B2}$$

$$S_N = \int d^2x\, d\tau \left(\frac{1}{2}(\partial_\mu N)^2 + \frac{r}{2}N^2 \right), \tag{B3}$$

$$S_{\psi,a} = \int d^2x\, d\tau\, \bar{\psi}[-i\gamma^\mu(\partial_\mu + iea_\mu)]\psi, \tag{B4}$$

$$S_{mixing} = \int d^2x\, d\tau\, i\bar{\psi}\vec{\sigma}\mu^z\psi\cdot(\lambda\vec{N}), \tag{B5}$$

$$S_h = \int d^2x\, d\tau\, \vec{h}\cdot(ai\bar{\psi}\vec{\sigma}\mu^z\psi + b\vec{N}). \tag{B6}$$

Here a and b are nonuniversal constants that depend on details of the microscopic physics.

Now by expanding the terms that contain $i\bar{\psi}\mu^z\vec{\sigma}\psi$ (one coming from S_{mixing} and one from coupling to the $\vec{h}$ field) up to quadratic order and performing the integral over ψ and a fields, we get the following form for the partition function:

$$Z = \int [DN] \exp\left(-S_N - b\int d^2x\, d\tau\, \vec{h}\cdot\vec{N} \right) \times \int d^2q\, d\omega \frac{\chi(q,\omega)}{2} |\vec{h} + \lambda\vec{N}|^2, \tag{B7}$$

where $\chi(q,\omega)$ is the susceptibility of the $i\bar{\psi}\vec{\sigma}\mu^z\psi$ operator

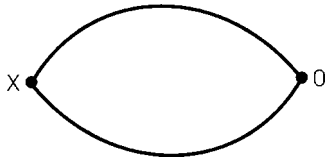

FIG. 8. Spin-spin correlation in mean field.

calculated using the action $S_{\psi,a}$. We can rewrite the $[\chi(q,\omega)/2]|\vec{h}+\lambda\vec{N}|^2$ up to quadratic order in N as an exponential. Putting this form in Eq. (B7) we get the following for the partition function:

$$Z = \int [DN] e^{-S_N^{eff}}, \tag{B8}$$

$$S_N^{eff} = S_N + \int d^2q\, d\omega \left(b\vec{h}_q\cdot\vec{N}_{-q} - \frac{\chi(q,\omega)}{2}|a\vec{h}_q + \lambda\vec{N}_q|^2 \right) = \int d^2q\, d\omega \left(\frac{\chi_N(\omega,q)^{-1}}{2}|\vec{N}_q|^2 + \vec{h}_q\cdot\vec{N}_{-q} - \frac{\chi(q,\omega)}{2}|\vec{h}+\lambda\vec{N}|^2 \right). \tag{B9}$$

Now to get the quadratic action for $\vec{h}$ field we should integrate out the $\vec{N}$ field, which is a simple Gaussian integral now. This leads to the following value for the effective susceptibility:

$$\chi_{eff} = \frac{a^2\chi + b^2\chi_N - 2\lambda ab\chi\chi_N}{1-\lambda^2\chi\chi_N}. \tag{B10}$$

You can see that as one expects, for $\lambda=0$, this reduces to the sum of the susceptibilities for $\vec{N}$ and $i\bar{\psi}\mu^z(\vec{\sigma}/2)\psi$ fields. Also note that this is valid only for the frequencies where $\lambda^2\chi\chi_N$ is not of order 1 (i.e., it is not valid for small frequencies). Now by analytic continuation to real frequencies and taking the imaginary part, we get the spectral functions plotted in sec. III A.

APPENDIX C: FEYNMAN DIAGRAMS

1. Spin-spin correlation in mean-field theory

For spin-spin correlation we need to calculate the following diagram which consists of two fermionic propagators. The fermionic propagator in the mean field is derived from the action (12):

$$\underset{p}{\text{—}} = \frac{1}{\not{p} - i\lambda\vec{N}\cdot\vec{\sigma}}. \tag{C1}$$

This diagram (Fig. 8), in the real space, corresponds to the following integral:

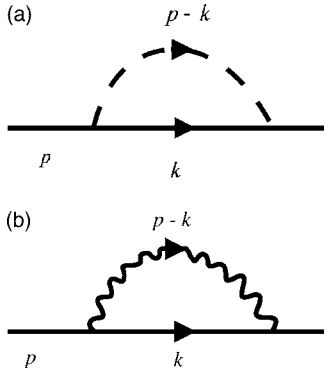

FIG. 9. Fermion self-energy.

$$\langle S_i S_j \rangle = -\delta_{ij} \int \frac{d^3p}{(2\pi)^3} \frac{d^3q}{(2\pi)^3} \times e^{-i\vec{p}\cdot\vec{r}} \frac{\mathrm{tr}[(\not{p}+\not{q}-i\lambda\vec{N}\cdot\vec{\sigma})(\not{q}-i\lambda\vec{N}\vec{\sigma})]}{[(p+q)^2+\lambda^2N^2](q^2+\lambda^2N^2)}. \quad \text{(C2)}$$

After integrating over q this gives

$$\langle S_i S_j \rangle \propto -\frac{\delta_{ij}}{r} \int p\, dp \sin(pr) \left[4\lambda N + \frac{2}{p} \arctan\left(\frac{p}{2\lambda N}\right) \times (4\lambda^2N^2+p^2) \right]. \quad \text{(C3)}$$

The first term is proportional to $\delta(r)$. Since we are interested in the case where $r \neq 0$, we can ignore that term. The second term gives

$$\frac{e^{-2\lambda N r}}{r^4}(1+2\lambda N r). \quad \text{(C4)}$$

We already saw that N goes to zero as g approaches g_c like $g_c - g$. So if we define the correlation length as $\xi = 1/2\lambda N$ we get Eqs. (13) and (14).

2. Beyond the mean field: ϵ expansion

Now to do the ϵ expansion we need to study the action given in Eq. (18). We can see that there are three different types of vertices present in the theory and 11 different one-loop diagrams which cause field renormalizations, vertex corrections, and mass renormalization. We use the following diagrammatic representation for the propagators of the fields in the theory:

$$\underset{p}{\overset{a}{\text{-------}}\overset{b}{}} = \frac{\delta^{ab}}{p^2+r}$$

$$\underset{p}{\text{———}} = \frac{1}{\not{p}}$$

$$\underset{p}{\overset{\mu}{\sim\sim\sim}\overset{\nu}{}} = \frac{\delta^{\mu\nu}}{p^2}. \quad \text{(C5)}$$

Here we have used Feynman gauge for the gauge-field propagator, and the Euclidean metric. Now we start to calculate the one-loop diagrams.

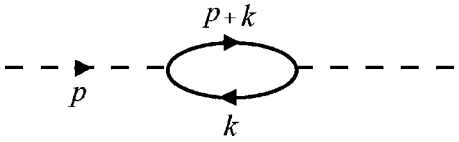

FIG. 10. N-field self-energy.

a. Fermion self-energy

There are two one-loop diagrams that will generated fermion self-energy. The diagram in Fig. 9(a) represents the N-field contribution to the fermion self-energy:

$$\Sigma_N^{\psi}\not{p} = (i\lambda)^2 \int \frac{d^dk}{(2\pi)^d} \sigma^j \frac{\delta^{ij}\not{k}}{k^2(k+p)^2} \sigma^j = -\frac{3}{(4\pi)^2}\frac{\lambda^2}{\epsilon}\not{p}. \quad \text{(C6)}$$

Figure 9(b) represents the gauge-field contribution to the fermion self-energy:

$$\Sigma_a^{\psi}\not{p} = e^2 \int \frac{d^dk}{(2\pi)^d} \gamma^\mu \frac{\delta^{\mu\nu}\not{k}}{k^2(k+p)^2} \gamma^\nu = -\frac{1}{(4\pi)^2}\frac{e^2}{\epsilon}\not{p}. \quad \text{(C7)}$$

b. N-field self-energy

Since the N field is coupled to the fermion field only, there is just one diagram contributing to its self-energy (Fig. 10). This has the following contribution:

$$\Sigma_{\psi}^N p^2 \delta^{ij} = (-1)(i\lambda)^2 \int \frac{d^dk}{(2\pi)^d} \frac{\mathrm{tr}(\sigma^i\sigma^j)\mathrm{tr}[\not{k}(\not{k}+\not{p})]}{k^2(k+p)^2} = -\frac{8}{(4\pi)^2}\frac{\lambda^2}{\epsilon}p^2\delta^{ij}. \quad \text{(C8)}$$

Here the minus sign appears because of the presence of a fermionic loop in the diagram.[49]

c. Gauge-field self-energy

The gauge field is only coupled to the fermion field as well, so there is only one diagram generating gauge-field self-energy (Fig. 11). This diagram has the following contribution:

$$\Sigma_{\psi}^a[p^\mu p^\nu - p^2\delta^{\mu\nu}] = (-1)e^2 \int \frac{d^dk}{(2\pi)^d} \frac{\mathrm{tr}[\gamma^\mu\not{k}\gamma^\nu(\not{k}+\not{p})]}{k^2(k+p)^2} = -\frac{16}{(4\pi)^2}\frac{e^2}{3\epsilon}p^2\left(\delta^{\mu\nu}-\frac{p^\mu p^\nu}{p^2}\right). \quad \text{(C9)}$$

Note that in this relation the term proportional to $p^\mu p^\nu$ dose not contribute to physical observables (S-matrix elements). This is guaranteed by the Ward identity.[49]

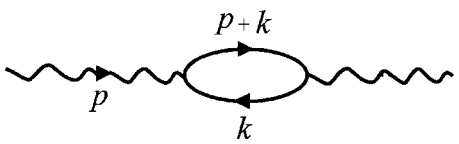

FIG. 11. Gauge-field self-energy.

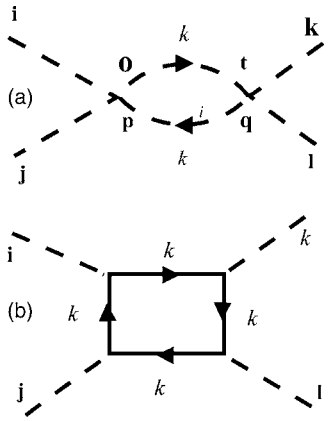

FIG. 12. u renormalization.

d. $u[(\vec{N})^2]^2$ vertex correction

There are two diagrams contributing to this vertex renormalization at the one-loop level. Note that up to one-loop order, it is enough to calculate vertex corrections with zero external momentum. The diagram of Fig. 12(a) gives

$$\begin{aligned}\Delta_N^u(\delta^{ij}\delta^{kl}+\delta^{ik}\delta^{jl}+\delta^{il}\delta^{jk})&=-\frac{u^2}{6}(\delta^{ij}\delta^{pp}+\delta^{io}\delta^{jp}+\delta^{ip}\delta^{jo})\\&\times\int\frac{d^dk}{(2\pi)^2}\frac{\delta^{oq}\delta^{pt}}{(k^2+r)^2}(\delta^{qt}\delta^{kl}+\delta^{qk}\delta^{tl}+\delta^{ql}\delta^{tk})\\&=-\frac{11}{(4\pi)^2}\frac{u^2}{3\epsilon}(\delta^{ij}\delta^{kl}+\delta^{ik}\delta^{jl}+\delta^{il}\delta^{jk}).\end{aligned}\tag{C10}$$

The contribution of Fig. 12(b) is similarly calculated:

$$\begin{aligned}\Delta_\psi^u(\delta^{ij}\delta^{kl}+\delta^{ik}\delta^{jl}+\delta^{il}\delta^{jk})&=-3(-1)(i\lambda)^4\int\frac{d^dk}{(2\pi)^d}\frac{\mathrm{tr}(\not{k}^4)}{k^8}\mathrm{tr}(\sigma^i\sigma^j\sigma^k\sigma^l)\\&=\frac{96}{(4\pi)^2}\frac{\lambda^4}{\epsilon}(\delta^{ij}\delta^{kl}+\delta^{ik}\delta^{jl}+\delta^{il}\delta^{jk}).\end{aligned}\tag{C11}$$

Again one minus sign appears because of the fermionic loop.[49]

e. N-ψ vertex correction

Again, there are two different diagrams associated with this correction at the one-loop level. As before we set the external momenta to zero. Then the contribution of the diagram of Fig. 13(a) is:

$$i\Delta_N^\lambda\sigma^k=(i\lambda)^3\int\frac{d^dk}{(2\pi)^d}\frac{\not{k}}{k^2}\sigma^j\frac{\delta^{ij}\sigma^k}{k^2+r}\sigma^j\frac{\not{k}}{k^2}=i\frac{2}{(4\pi)^2}\frac{\lambda^3}{\epsilon}\sigma^k\tag{C12}$$

and the diagram in Fig. 13(b) gives

$$i\Delta_a^\lambda=i\lambda e^2\int\frac{d^dk}{(2\pi)^d}\frac{\not{k}}{k^2}\gamma^\mu\frac{\delta^{\mu\nu}}{k^2+r}\gamma^\nu\frac{\not{k}}{k^2}=i\frac{6}{(4\pi)^2}\frac{\lambda e^2}{\epsilon}.\tag{C13}$$

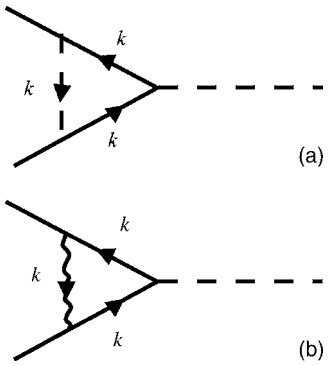

FIG. 13. λ renormalization.

f. a-ψ vertex correction

As in Appendix C 2 e there are two diagrams. The first diagram [Fig. 14(a)] gives

$$\Delta_a^e\gamma^\alpha=e^3\int\frac{d^dk}{(2\pi)^d}\gamma^\mu\frac{\not{k}}{k^2}\frac{\gamma^\alpha\delta^{\mu\nu}}{k^2}\frac{\not{k}}{k^2}\gamma^\nu=\frac{1}{(4\pi)^2}\frac{e^3}{\epsilon}\gamma^\alpha\tag{C14}$$

and Fig. 14(b) gives

$$\Delta_N^e\gamma^\alpha=e(i\lambda)^2\int\frac{d^dk}{(2\pi)^d}\sigma^i\frac{\not{k}}{k^2}\frac{\gamma^\alpha\delta^{ij}}{k^2+r}\frac{\not{k}}{k^2}\sigma^j=\frac{3}{(4\pi)^2}\frac{e^3}{\epsilon}\gamma^\alpha.\tag{C15}$$

Note that Eq. (C14) is minus the contribution of Eq. (C7) and Eq. (C15) has the negative contribution of Eq. (C6). This, in fact, should be the case to keep gauge invariance of the theory.

g. Mass renormalization

The last one-loop diagram we consider generates mass renormalization:

$$\begin{aligned}\Delta_r\delta^{ij}&=\frac{u}{6}(\delta^{ij}\delta^{kl}+\delta^{ik}\delta^{jl}+\delta^{il}\delta^{jk})\int\frac{d^dk}{(2\pi)^d}\frac{\delta^{lk}}{k^2+r}\\&=-\frac{5}{(4\pi)^2}\frac{u}{3\epsilon}\delta^{ij},\end{aligned}\tag{C16}$$

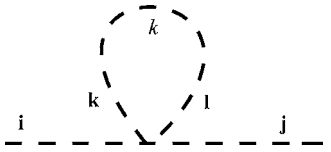

3. Renormalization conditions

Now with these in hand, we can proceed using the minimal subtraction scheme. Introducing a mass scale $m\propto\sqrt{r}$ we can write the following set of renormalization conditions:

$$\not{p}(Z_\psi-(\Sigma_N^\psi+\Sigma_a^\psi))=\text{finite } O\text{ (2 loops)},$$

$$m^{-\epsilon/2}e_0Z_\psi\sqrt{Z_a}+(\Delta_N^e+\Delta_a^e)=\text{finite } O\text{ (2 loops)},$$

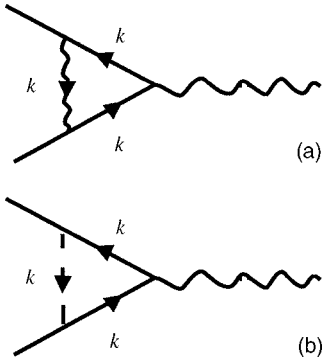

FIG. 14. e renormalization.

$$Z_N(p^2+r)+(r\Delta_r-\Sigma_\psi^N p^2)=\text{finite } O\ (2\text{ loops}),$$

$$m^{-\epsilon/2}\lambda_0 Z_\psi\sqrt{Z_N}+(\Delta_N^\lambda+\Delta_a^\lambda)=\text{finite } O\ (2\text{ loops}),$$

$$p^2(Z_a-\Sigma_\psi^a)=\text{finite } O\ (2\text{ loops}),$$

$$m^{-\epsilon}u_0 Z_N^2+(\Delta_N^u+\Delta_\lambda^u)=\text{finite } O\ (2\text{ loops}).$$

Here e_0, λ_0, and u_0 are bare coupling constants and so do not flow with the mass scale. These relations give field renormalization coefficients directly, since the divergence part of the self-energy diagrams should cancel out with these field renormalization coefficients:

$$Z_\psi=1+\Sigma_\psi^N+\Sigma_\psi^a, \tag{C17}$$

$$Z_N=1+\Sigma_N^\psi, \tag{C18}$$

$$Z_a=1+\Sigma_a^\psi. \tag{C19}$$

Putting them back in the renormalization condition equations, and letting the mass scale flow,[49] we get the equations given in Sec. V.

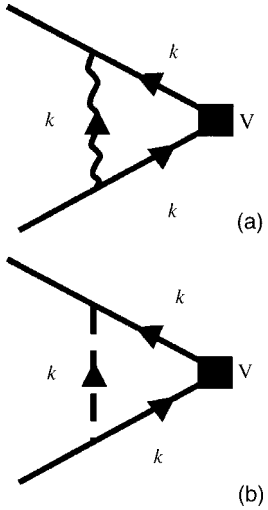

FIG. 15. Bilinear operator scaling dimension.

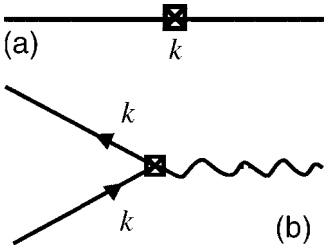

FIG. 16. Velocity anisotropy vertices.

4. Renormalization of bilinear operators

Here we introduce a new term in the Lagrangian with the general form

$$v\bar{\psi}\mathcal{O}\psi, \tag{C20}$$

where $\mathcal{O}$ is the combination of μ and σ matrices that are given in Table I. There are two new diagrams corresponding to this new vertex [Figs. 15(a) and 15(b)]. Diagram 15(a) gives

$$\Delta_\mathcal{O}^N\mathcal{O}=(i\lambda)^2\int\frac{d^dk}{(2\pi)^d}\sigma^j\mu^z\frac{\not{k}}{k^2}\mathcal{O}\frac{\not{k}}{k^2}\frac{\delta^{ij}}{k^2+r}\mu^z\sigma^j$$

$$=-\lambda^2\frac{2}{(4\pi)^2\epsilon}A_\mathcal{O}\mathcal{O},\quad A_\mathcal{O}\mathcal{O}=\sigma^j\mu^z\mathcal{O}\mu^z\sigma^j, \tag{C21}$$

and diagram 15(b) gives

$$\Delta_\mathcal{O}^a\mathcal{O}=e^2\int\frac{d^dk}{(2\pi)^d}\gamma^\mu\frac{\not{k}}{k^2}\mathcal{O}\frac{\not{k}}{k^2}\frac{\delta^{\mu\nu}}{k^2}\gamma^\nu=e^2\frac{6}{(4\pi)^2\epsilon}\mathcal{O}. \tag{C22}$$

With these in hand we can get the scaling dimension of v:

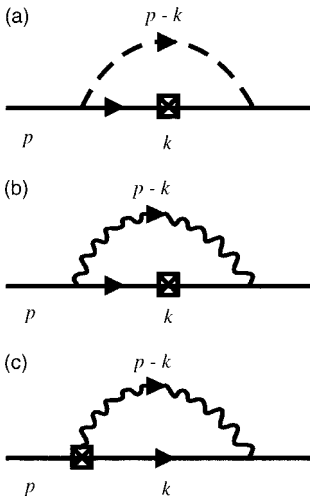

FIG. 17. Velocity anisotropy one-loop renormalization.

$$\Delta_v = 1 + \delta_v = [1 + (\Delta_{\mathcal{O}}^N + \Sigma_{\psi}^N)\lambda^2 + (\Delta_{\mathcal{O}}^a + \Sigma_{\psi}^a)e^2]v$$
$$= \left(1 + (-2A_{\mathcal{O}} - 3)\frac{\lambda^2}{(4\pi)^2} + 5\frac{e^2}{(4\pi)^2}\right)v. \quad \text{(C23)}$$

This gives the scaling dimension of $v(1+\delta_v)$. Now to get the scaling dimension of $\mathcal{O}(\Delta_{\mathcal{O}})$, note that

$$\Delta_{\mathcal{O}} = D - (1 + \delta_v) = 3 - \epsilon - \delta_v. \quad \text{(C24)}$$

Using the fixed point values for λ and e, we get the scaling dimensions mentioned in Table I.

5. Velocity anisotropy

In this section we assume a small velocity anisotropy and treat it as a perturbation to our QED_3 theory. Following the notation used in Ref. 30, this anisotropy is presented by

$$K_a = -i\delta\bar{\psi}\mu^z\hat{\gamma}^{\mu}(\partial_{\mu} + iea_{\mu})\psi. \quad \text{(C25)}$$

Here, δ is the small perturbation parameter (we are essentialy interested in its behavior under renormalization) and $\hat{\gamma}^{\mu} = \gamma^x\delta_{x,\mu} - \gamma^y\delta_{y,\mu}$. There are two vertices associated with this perturbation. One is the correction in fermionic kinetic energy presented in Fig. 16(a) and the correction to the a-ψ vertex presented in Fig. 16(b):

$$-\delta\mu^z\hat{\not{k}}, \quad \text{(C26)}$$

$$-\delta\mu^z\hat{\not{\gamma}}^{\mu}, \quad \text{(C27)}$$

So there are three different types of one-loop diagrams in addition to the field renormalization factors calculated before contributing renormalization of the anisotropy term in the fermionic kinetic energy (i.e., δ). The diagram in Fig. 17(a) gives

$$-\delta\Sigma_{\delta}^N\hat{\not{p}} = -\delta(i\lambda)^2\int\frac{d^dk}{(2\pi)^d}\sigma^i\frac{1}{\not{k}}\hat{\not{k}}\frac{1}{\not{k}}\frac{\delta^{ij}}{(p-k)^2 + r}\sigma^j$$
$$= -\frac{\delta}{(4\pi)^2}\frac{\lambda^2}{\epsilon}\hat{\not{p}}. \quad \text{(C28)}$$

The diagram of Fig. 17(b) similarly gives

$$-\delta\Sigma_{\delta}^a\delta\hat{\not{p}} = -\delta e^2\int\frac{d^dk}{(2\pi)^d}\gamma^{\mu}\frac{1}{\not{k}}\hat{\not{k}}\frac{1}{\not{k}}\frac{\delta^{\mu\nu}}{(p-k)^2}\gamma^{\nu} = -\frac{\delta}{3(4\pi)^2}\frac{e^2}{3\epsilon}\hat{\not{p}}. \quad \text{(C29)}$$

The diagram of Fig. 17(c) and the similar one with the correction on the right vertex give

$$-\delta\Delta_{\delta}^a\hat{\not{p}} = \delta e^2\int\frac{d^dk}{(2\pi)^d}\hat{\gamma}^{\mu}\frac{1}{\not{k}}\frac{\delta^{\mu\nu}}{(p-k)^2}\gamma^{\nu} = \frac{\delta}{(4\pi)^2}\frac{2e^2}{\epsilon}\hat{\not{p}}. \quad \text{(C30)}$$

Now with these and also the field renormalization coefficients calculated previously we can get the RG flow for δ:

$$\beta_{\delta} = \delta(2\Delta_{\delta}^a + \Sigma_{\delta}^N + \Sigma_{\delta}^a + \Sigma_N^{\psi} + \Sigma_a^{\psi})$$
$$= -\delta\left(\frac{14}{3(4\pi)^2}e^2 + \frac{2}{(4\pi)^2}\lambda^2\right). \quad \text{(C31)}$$

This proves that the small velocity anisotropy is irrelevant.

[1] J. Orenstein and A. J. Millis, Science **288**, 468 (2000).
[2] H. A. Mook, M. Yethiraj, G. Aeppli, T. E. Mason, and T. Armstrong, Phys. Rev. Lett. **70**, 3490 (1993).
[3] H. F. Fong, B. Keimer, D. L. Milius, and I. A. Aksay, Phys. Rev. Lett. **78**, 713 (1997).
[4] H. He, Y. Sidis *et al.*, Phys. Rev. Lett. **86**, 1610 (2001).
[5] A. V. Chubukov, S. Sachdev, and J. Ye, Phys. Rev. B **49**, 11919 (1994).
[6] D. K. Morr and D. Pines, Phys. Rev. Lett. **81**, 1086 (1998).
[7] M. Vojta, C. Buragohain, and S. Sachdev, Phys. Rev. B **61**, 15152 (2000).
[8] H. F. Fong, P. Bourges, Y. Sidis, L. P. Regnault, J. Bossy, A. Ivanov, D. L. Milius, I. A. Aksay, and B. Keimer, Phys. Rev. B **61**, 14773 (2000).
[9] P. Dai, H. A. Mook, R. D. Hunt, and F. Doğan, Phys. Rev. B **63**, 054525 (2000).
[10] P. W. Anderson, Science **235**, 1196 (1987).
[11] S. A. Kivelson, D. S. Rokhsar, and J. P. Sethna, Phys. Rev. B **35**, 8865 (1987).
[12] N. Read and S. Sachdev, Phys. Rev. Lett. **62**, 1694 (1989).
[13] S. Sachdev, Phys. Rev. B **40**, 5204 (1989).
[14] N. Read and S. Sachdev, Phys. Rev. Lett. **66**, 1773 (1991).
[15] S. Sachdev, Rev. Mod. Phys. **75**, 913 (2003).
[16] D. Z. Liu, Y. Zha, and K. Levin, Phys. Rev. Lett. **75**, 4130 (1995).
[17] A. J. Millis and H. Monien, Phys. Rev. B **54**, 16172 (1996).
[18] A. Abanov and A. V. Chubukov, Phys. Rev. Lett. **83**, 1652 (1999).
[19] M. R. Norman, Phys. Rev. B **61**, 14751 (2000).
[20] J. Brinckmann and P. A. Lee, Phys. Rev. B **65**, 014502 (2002).
[21] E. W. Carlson, V. J. Emery, S. A. Kivelson, and D. Orgad, in *Physics of Conventional and Unconventional Superconductors*, edited by K. H. Bennemann and J. B. Ketterson (Springer, Berlin, 2003).
[22] T. Senthil and M. P. A. Fisher, Phys. Rev. B **62**, 7850 (2000).
[23] M. Hermele, T. Senthil, M. P. A. Fisher, P. A. Lee, N. Nagaosa, and X.-G. Wen, Phys. Rev. B **70**, 214437 (2004).
[24] I. Affleck and J. B. Marston, Phys. Rev. B **37**, R3774 (1988).
[25] J. B. Marston and I. Affleck, Phys. Rev. B **39**, 11538 (1989).
[26] X.-G. Wen and P. A. Lee, Phys. Rev. Lett. **76**, 503 (1996).
[27] D. H. Kim and P. A. Lee, Ann. Phys. (N.Y.) **272**, 130 (1999).
[28] W. Rantner and X.-G. Wen, Phys. Rev. B **66**, 144501 (2002).
[29] T. Senthil and P. A. Lee, Phys. Rev. B **71**, 174515 (2005).
[30] M. Hermele, T. Senthil, and M. P. A. Fisher, Phys. Rev. B **72**, 104404 (2005).
[31] S. Sachdev and K. Park, Ann. Phys. (N.Y.) **298**, 58 (2002).

[32] T. C. Hsu, Phys. Rev. B **41**, 11379 (1990).
[33] L. Balents, M. P. A. Fisher, and C. Nayak, Phys. Rev. B **60**, 1654 (1999).
[34] T. Senthil and M. P. A. Fisher, Phys. Rev. B **63**, 134521 (2001a).
[35] T. Senthil and M. P. A. Fisher, in *More is Different: Fifty Years of Condensed Matter Physics*, edited by N. P. Ong and R. N. Bhatt (Princeton University Press, Oxford, 2001).
[36] C.-M. Ho, V. N. Muthukumar, M. Ogata, and P. W. Anderson, Phys. Rev. Lett. **86**, 1626 (2001).
[37] T. Senthil, A. Vishwanath, L. Balents, S. Sachdev, and M. P. A. Fisher, Science **303**, 1490 (2004a).
[38] T. Senthil, L. Balents, S. Sachdev, A. Vishwanath, and M. P. A. Fisher, Phys. Rev. B **70**, 144407 (2004b).
[39] W. Rantner and X.-G. Wen, Phys. Rev. Lett. **86**, 3871 (2001).
[40] D. A. Ivanov, Ph.D. thesis, MIT, 2000.
[41] A. Paramekanti, M. Randeria, and N. Trivedi, Phys. Rev. B **71**, 094421 (2005).
[42] C. Gros, Ann. Phys. (N.Y.) **189**, 53 (1988).
[43] T. K. Lee and C. T. Shih, Phys. Rev. B **55**, 5983 (1997).
[44] L. Balents, M. P. A. Fisher, and C. Nayak, Int. J. Mod. Phys. B **12**, 1033 (1998).
[45] J. Zinn-Justin, *Quantum Field Theory and Critical Phenomena* (Oxford University Press, New York, 1993).
[46] O. Vafek, Z. Tesanovic, and M. Franz, Phys. Rev. Lett. **89**, 157003 (2002).
[47] M. Franz, Z. Tesanovic, and O. Vafek, Phys. Rev. B **66**, 054535 (2002).
[48] D. J. Lee and I. F. Herbut, Phys. Rev. B **66**, 094512 (2002).
[49] M. E. Peskin and D. V. Schroeder, *An Introduction to Quantum Field Theory* (Perseus Books Publishing, Cambridge, MA, 1995).
[50] P. A. Lee, N. Nagaosa, and X.-G. Wen, cond-mat/0410445 (unpublished).
[51] Note that if $\vec{N}=N_0\hat{z}$, then S^z is a good quantum number and can be used to label the states. The spinons have $S^z=\pm 1/2$.
[52] It is at present not known what the value of N_c is though existing numerical work suggests the bound $N_c<8$. For the SU(2) magnet studied in this paper we have $N=4$ and have simply assumed that $N_c<4$.